JOC Article

Exchange Interaction of 5,5′-(*m*- and *p*-Phenylene)bis(10-phenyl-5,10-dihydrophenazine) Dications and Related Analogues

Eriko Terada, Toshihiro Okamoto, Masatoshi Kozaki, Miyuki Eiraku Masaki, Daisuke Shiomi, Kazunobu Sato, Takeji Takui, and Keiji Okada*

Departments of Chemistry and Materials Science, Graduate School of Science, Osaka City University, Sugimoto, Sumiyoshi-ku, Osaka 558-8585, Japan

okadak@sci.osaka-cu.ac.jp

Received August 25, 2005

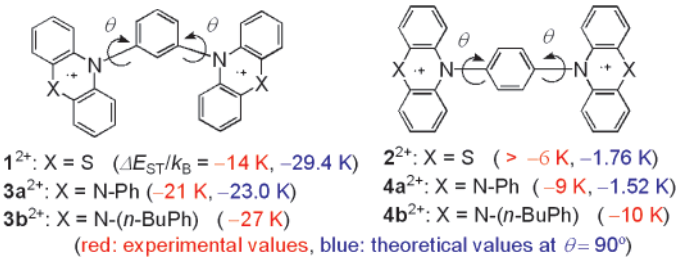

5,5′-(*m*-Phenylene)bis[(10-aryl-5,10-dihydrophenazine) dications, **3a**$^{2+}$ and **3b**$^{2+}$, and their *p*-analogues **4a**$^{2+}$ and **4b**$^{2+}$, were prepared, and their exchange interaction was investigated. The EPR spectra of these dications at 123 K in a butyronitrile matrix showed the population of a triplet state. The temperature dependence of the EPR signal intensity ($|\Delta m_s| = 2$) showed that these dications had singlet ground states with $\Delta E_{ST}/k_B = -27$ to -21 K for the *m*-isomer **3**$^{2+}$ and with $\Delta E_{ST}/k_B = -10$ to -8 K for the *p*-isomer **4**$^{2+}$. Theoretical calculation of the exchange interaction *J* for these dications at the orthogonal torsion angle geometries was carried out for **3a**$^{2+}$ and **4a**$^{2+}$ and for (*m*- and *p*-phenylene)bisphenothiazine dications **1**$^{2+}$ and **2**$^{2+}$ using the broken-symmetry approach for the singlet states. A good correlation was observed between the calculated *J* and a MO-energy term in the triplet state, $\Delta E_{TMO} = |\mathrm{HOMO}(\alpha) - (\mathrm{HOMO} - 1)(\alpha)|$. The calculated *J* values were negative in the order of 10 K for the *m*-dications ($J/k_B = -14.7$ K for **1**$^{2+}$, -11.5 K for **3a**$^{2+}$), but much smaller negative values were found for the *p*-isomers ($J/k_B = -0.9$ K for **2**$^{2+}$, -0.8 K for **4a**$^{2+}$). The smaller $|J|$ values for the *p*-dications are qualitatively consistent with the experimental ΔE_{ST} ($2J$) values.

Introduction

Understanding the magnetic interaction between unpaired electrons in organic molecules is one of the most fundamental and important subjects in the area of molecular magnetism.[1] In alternant hydrocarbon high-spin molecules, it is generally accepted that the *m*-phenylene or benzene-1,3,5-triyl connection of spin sources gives rise to a high-spin ground state, whereas the *p*-connection gives a low-spin ground state. Many experiments and theories have supported this rule.[1,2] Extension of this rule, for instance, the *m*-phenylene connection, to various systems other than alternant hydrocarbon spin sources has frequently succeeded.[1,2] However, recent studies have clearly shown that there exist some low-spin diradical systems[3] with the *m*-phenylene linkage.[2a,3] Rajca's group has demonstrated that even a Schlenk-type

* To whom correspondence should be addressed. Tel: +81-6-6605-2568. Fax: +81-6-6690-2709.

(1) (a) Lahti, P. M. In *Molecular-Based Magnetic Materials*; Turnbull, M. M., Sugimoto, T., Thompson, L. K., Eds.; American Chemical Society: Washington, DC, 1996; ACS Symposium Series 644, pp 218–235. (b) In *Magnetic Properties of Organic Materials*; Lahti, P. M., Ed.; Marcel Dekker: New York, 1999. (c) Amabilino, D. B.; Veciana, J. In *Magnetism: Molecules to Materials II*; Miller, J. S., Drillon, M., Eds.; Wiley-VCH: New York, 2001; pp 1–60. (d) Itoh, K., Kinoshita, M., Eds. *Molecular Magnetism*; Kodansha-Gordon and Breach: Tokyo, 2000. (e) Rajca, A. *Chem. Rev.* **1994**, *94*, 871–893.

(2) (a) Okada, K. In *Molecular Magnetism*; Itoh, K., Kinoshita, M., Eds.; Kodansha and Gordon and Breach: Tokyo, 2000; pp 264–277. (b) Borden, W. T., Iwamura, H., Berson, J. A. *Acc. Chem. Res.* **1994**, *27*, 109–116.

(3) (a) Dvolaitzky, M.; Chiarelli, R.; Rassat, A. *Angew. Chem., Int. Ed. Engl.* **1992**, *31*, 180–181. (b) Kanno, F.; Inoue, K.; Koga, N.; Iwamura, H. *J. Am. Chem. Soc.* **1993**, *115*, 847–850. (c) Fujita, J.; Tanaka, M.; Suemune, H.; Koga, N.; Matsuda, K.; Iwamura, H. *J. Am. Chem. Soc.* **1996**, *118*, 9347–9351.

10.1021/jo051791w CCC: $30.25
Published on Web 11/03/2005

alternant hydrocarbon diradical shows a low-spin ground state when the spin sources are linked by a sterically hindered 2,4,6-trimethyl-*m*-phenylene group.[4] Although such a low-spin ground state with the *m*-phenylene linkage is a rare case in alternant hydrocarbons, a larger number of low-spin species with the *m*-phenylene linkage have been observed in the system containing heteroatomic spin sources,[2a,3,5] in most cases of which the lone pair electrons of heteroatoms directly participate in the spin delocalization, i.e., heteroatoms are located with sp^3-hybridization at an even numbered position referenced to the formal spin center at position 1 as shown in **A** and **B** as examples, giving a nonalternant spin structure.[2a,6]

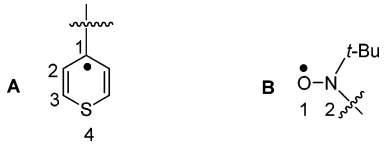

For instance, (2,4,6-trimethyl-*m*-phenylene)-[3a] or (4,6-dimethoxy-*m*-phenylene)bis(*tert*-butylnitroxide)s[3b] have singlet ground states, whereas the (*m*-phenylene)bis(*tert*-butylnitroxide) has a triplet ground state.[7] (*m*-Phenylene)bisphenothiazine dication $\mathbf{1}^{2+}$ has also a singlet ground state with a singlet−triplet energy gap, ΔE_{ST}, of ca. −14 K.[8] A similar result has been observed in a pyridinyl diradical.[9] Furthermore, there are some diradicals that exist as an equilibrium between conformational isomers, whose exchange interaction is conformation-dependent.[10,12b] Borden and co-workers have shown the importance of the dihedral angle between the spin sources and the *m*-phenylene spacer by theoretical calculation of (*m*-phenylene)bisnitroxide; the two nitroxide radical orbitals (magnetic orbitals) interact through the σ-bonds of the *m*-phenylene moiety at the perpendicular geometry, where the selective destabilization of the antisymmetric combination of the magnetic orbitals occurs, resulting in a singlet ground state.[11] Nowadays, the importance of the dihedral angles between the *m*-phenylene linker and the spin sources seems to be well established. More recently, an additional factor that affects the exchange interaction has also been reported. Shultz's group has experimentally shown that the exchange interaction can be altered by a remote substituent in 5-substituted *m*-phenylene diradicals.[12a] We have shown that (*m*-phenylene)bisxanthyl has a triplet ground state or a singlet ground state with a nearly degenerate triplet state, whereas the sulfur analogue (*m*-phenylene)-bisthioxantyl clearly has a singlet in the ground state.[6] These studies indicate that the spin density change caused by the substituents or heteroatoms also has an important role in the exchange interaction. It is likely that these two factors, dihedral angle and spin density, cooperatively affect the magnetic interaction of unpaired electrons for weakly coupled spin systems.[12b,c]

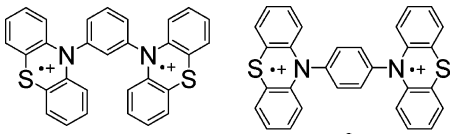

We have shown that some symmetrically[13] substituted (*p*-phenylene)-derived diradicals have triplet energies as low as that of the singlet states.[2a] 1,1′-(*p*-Phenylene)bis-(2,4,6-triphenylpyridinyl) diradical has a singlet ground state with a small $\Delta E_{ST}/k_B$ = ca. −26 K.[9] 10,10′-(*p*-Phenylene)bisphenothiazine dication $\mathbf{2}^{2+}$ generated in *c*-sulfuric acid affords a straight line in the Curie plots in temperatures down to 6 K, indicating that the ground state is a triplet state or a singlet state with $|\Delta E_{ST}/k_B| <$ ∼6 K.[8a] Similar observation has been reported for (*p*-phenylene)bis[2,5-di(2-thienyl)-1-pyrrole] dication by Juliá and co-workers.[14] These compounds have again a large dihedral angle and a nonalternant spin distribution nature in the spin source.[2a] A large dihedral angle certainly decreases the energy gap of two magnetic orbitals by breaking the π-network. Furthermore, the orbital interaction through the σ-bonds may be rather weak, simply because the spin sources are separated by the longer five σ-bonds in the *p*-phenylene isomers compared to four σ-bonds in the *m*-phenylene isomers. In addition, the spin density at the (benzylic nitrogen) spin center is diluted by the spin-delocalization. These factors contribute to placing the two magnetic orbitals for the *p*-phenylene dications in nearly degenerate levels. Under these circumstances, their nondisjoint nature[15] caused by the weak π (spin source)−σ (phenylene)−π (spin source) interaction may exert electronic repulsion in the singlet states to give triplet ground states with small positive *J* 's or to give singlet ground states with

(4) Rajca, A.; Rajca, S. *J. Chem. Soc., Perkin Trans. 2* **1998**, 1077−1082.

(5) Similar argument in phenylene-bridged bis(chloromethylene): (a) Zuev, P. S.; Sheridan, R. S. *J. Org. Chem.* **1994**, *59*, 2267−2269. (b) Zuev, P.; Sheridan, R. S. *J. Am. Chem. Soc.* **1993**, *115*, 3788−3789. (c) Trindle, C.; Datta, S. N.; Mallik, B. *J. Am. Chem. Soc.* **1997**, *119*, 12947−12951.

(6) Okada, K.; Imakura, T.; Oda, M.; Kajiwara, A.; Kamachi, M.; Yamaguchi, M. *J. Am. Chem. Soc.* **1997**, *119*, 5740−5741.

(7) Calder, A.; Forrester, A. R.; James, P. G.; Luckhurst, G. R. *J. Am. Chem. Soc.* **1969**, *91*, 3724−3727.

(8) (a) Okada, K.; Imakura, T.; Oda, M.; Murai, H.; Baumgarten, M. *J. Am. Chem. Soc.* **1996**, *118*, 3047−3048. (b) Okada, K.; Imakura, T.; Oda, M.; Kajiwara, A.; Kamachi, M.; Sato, K.; Shiomi, D.; Takui, T.; Itoh, K.; Gherghel, L.; Baumgarten, M. *J. Chem. Soc., Parkin Trans. 2* **1997**, 1059−1060.

(9) Okada, K.; Matsumoto, K.; Oda, M.; Akiyama, K.; Ikegami, Y. *Tetrahedron Lett.* **1997**, *38*, 6007−6010.

(10) Conformational dependence of the ground states: (a) Shultz, D. A. In *Magnetic Properties of Organic Materials*; Lahti, P. M., Ed.; Marcel Dekker: New York, 1999; pp 103−125. (b) Rajca, A.; Lu, K.; Rajca, S.; Roth, C. R., II. *Chem. Commun.* **1999**, 1249−1250. (c) Nakai, T.; Kozaki, M.; Sato, K.; Shiomi, D.; Takui, T.; Itoh, K.; Okada, K. *Mol. Cryst. Liq. Cryst.* **1999**, *334*, 139−148.

(11) Fang, S.; Lee, M.-S.; Hrovat, D. A.; Borden, W. T. *J. Am. Chem. Soc.* **1995**, *117*, 6727−6731.

(12) (a) Shultz, D. A.; Bodnar, S. H.; Lee, H.; Kampf, J. W.; Incarvito, C. D.; Rheingold, A. L. *J. Am. Chem. Soc.* **2002**, *124*, 10054−10061. (b) Shultz, D. A.; Fico, R. M., Jr.; Bodnar, S. H.; Kumar, R. K.; Vostrikova, K. E.; Kampf, J. W.; Boyle, P. D. *J. Am. Chem. Soc.* **2003**, *125*, 11761−11771. (c) Shultz, D. A.; Fico, R. M., Jr.; Lee, H.; Kampf, J. W.; Kirschbaum, K.; Pinkerton, A. A.; Boyle, P. D. *J. Am. Chem. Soc.* **2003**, *125*, 15426−15432.

(13) Some asymmetrically substituted high-spin diradicals of the type of 4-(2-allyl)benzyl diradicals have been reported: (a) Inoue, K.; Iwamura, H. *Angew. Chem., Int. Ed. Engl.* **1995**, *34*, 927−928. (b) Kumai, R.; Sakurai, H.; Izuoka, A.; Sugawara, T. *Mol. Cryst. Liq. Cryst.* **1996**, *279*, 133−138. (c) Ishiguro, K.; Ozaki, M.; Kamekura, Y.; Sekine, N.; Sawaki, Y. *Mol. Cryst. Liq. Cryst.* **1997**, *306*, 75−80.

(14) Domingo, V. M.; Alemán, C.; Brillas, E.; Juliá, L. *J. Org. Chem.* **2001**, *66*, 4058−4061.

(15) Borden, W. T.; Davidson, E. R. *J. Am. Chem. Soc.* **1977**, *99*, 4587−4594.

SCHEME 1

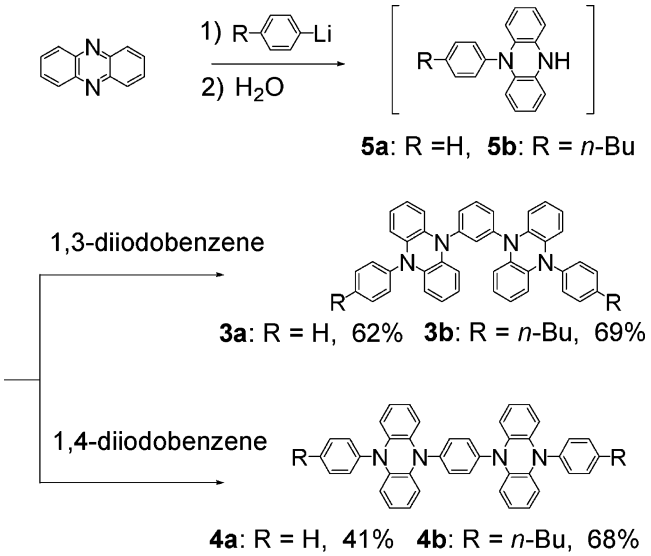

small negative J's, depending on the degree of degeneracy of the magnetic orbitals.

To obtain more insight into this subject, we required a pure sample of 10,10′-(*p*-phenylene)bisphenothiazine dication $\mathbf{2}^{2+}$. Recently, Kochi and co-workers described the isolation of dication $\mathbf{2}^{2+}$.[16] We have also attempted the isolation of $\mathbf{2}^{2+}$. Treatment of a CH_2Cl_2 solution of compound **2** with a large excess amount of $SnCl_5$ gave a dicationic species as precipitates. The isolated species showed a satisfactory elemental analysis as $C_{30}H_{20}N_2S_2 \cdot 2SbCl_6$ within ±0.3% and exhibited a triplet EPR pattern similar to that reported in *c*-sulfuric acid.[8a] However, the species showed a comparably strong signal due to the monoradical cation $\mathbf{2}^{+}$ as an impurity. Therefore, we altered the structure of the spin source to a much more readily oxidizable dihydrophenazine framework.[17] We report the synthesis and exchange interaction of 5,5′-(*m*- and *p*-phenylene)bis[10-phenyl- and 10-(4-*n*-butylphenyl)-5,10-dihydrophenazine] dications, $\mathbf{3}^{2+}$ and $\mathbf{4}^{2+}$. Theoretical analysis of the exchange interaction of these dications and the related (*m*- and *p*-phenylene)bisphenothiazine dications, $\mathbf{1}^{2+}$ and $\mathbf{2}^{2+}$, at the perpendicular geometry is also provided.

Results and Discussion

Synthesis and Oxidation Potential. We have recently developed a convenient method for the synthesis of unsymmetrical 5,10-diaryl-substituted 5,10-dihydrophenazines.[17a] The synthesis of 5,5′-(*m*- or *p*-phenylene)-bis(10-diphenyl-5,10-dihydrophenazine) derivatives is shown in Scheme 1. The key step, in situ preparation of 5-phenyl or 5-(4-*n*-butylphenyl)-5,10-dihydrophenazine (**5a** or **5b**), involves the following processes under a nitrogen atmosphere: the addition of aryllithium to a solution of phenazine in *o*-xylene or toluene, quenching with water, and drying the organic layer. The monosubstituted 5,10-dihydrophenazine **5** is unstable under aerated conditions. However, the solution of **5** under a nitrogen atmosphere can be kept in a freezer for months as a stock solution. The cross-coupling reaction of **5** (2.5 equiv) with *m*- or *p*-diiodobenzene (1 equiv) using Pd(dba)$_2$−NaO^{t}Bu-P(^{t}Bu)$_3$ as a catalytic system gave **3a**,**b** or **4a**,**b** in moderate yields (Scheme 1, yield based on the diiodobenzene). The *p*-phenylene-linked 10,10′-diphenyl derivative **4a** had poor solubility in various organic solvents and was inconvenient for the preparation of the dication. Therefore, a detailed study was carried out on the 4-*n*-butylphenyl dications $\mathbf{3b}^{2+}$, $\mathbf{4b}^{2+}$. Some EPR and the temperature dependence data for $\mathbf{3a}^{2+}$, $\mathbf{4a}^{2+}$ are provided as Supporting Information.

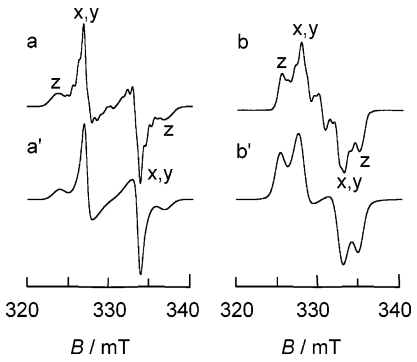

FIGURE 1. EPR spectra for $\mathbf{3b}^{2+}$ (a) and $\mathbf{4b}^{2+}$ (b) in butyronitrile at 123 K and their simulation spectra using a simulation program, WINEPR Simfonia ($\mathbf{3b}^{2+}$: $D/hc = 0.00598$ cm^{-1}, $E/hc = 0$ cm^{-1} (**a**′). $\mathbf{4b}^{2+}$: $D/hc = 0.00437$ cm^{-1}, $E/hc = 0$ cm^{-1} (**b**′).

The neutral compounds showed two reversible peaks at low potentials [+0.33 and +1.04 V (vs SCE) for **3a**, +0.32 and +1.02 for **4a**, +0.28 and ca. +1.0 (adsorption peak) for **3b**, +0.27 and ca. +0.9 (adsorption peak) for **4b** in DMF in the presence of tetrabutylammonium perchlorate (0.1 M)] (Figure S1). Semiderivative voltammetry of **3a** confirms that each peak involves sequential two-electron oxidation processes (Figure S1). The neutral compounds **3** and **4** were oxidized using tris(*p*-bromophenyl)aminium hexachloroantimonate (2 equiv, reduction potential +1.18 V) in acetonitrile or acetonitrile−THF in a glovebox. The oxidized solution was concentrated to the minimum amount. Addition of an excess amount of dry ether gave fine green precipitates. Recrystallization from an acetonitrile−benzene mixture gave green crystals, whose elemental analysis was in accord with the expected dications, $\mathbf{3b}^{2+}(SbCl_6^-)_2 \cdot C_6H_6$ and $\mathbf{4b}^{2+}(SbCl_6^-)_2$.

EPR Studies for 5,5′-(*m*- and *p*-Phenylene)bis[10-(4-butylphenyl)-5,10-dihydrophenazine] Dications, $\mathbf{3b}^{2+}$ and $\mathbf{4b}^{2+}$. Figure 1 shows the EPR spectra in a butyronitrile matrix at 123 K for the isolated $\mathbf{3b}^{2+}$ and $\mathbf{4b}^{2+}$ with the simulation spectra. The observed signals showed a typical pattern of randomly oriented triplet species with overlapping nitrogen hyperfine couplings in *x*,*y* components. Only a small signal of impurity due to $\mathbf{3b}^{+}$ or $\mathbf{4b}^{+}$ appears in the center field. The hyperfine splittings were disregarded and treated as line-broadening in the simulation spectra. The fine structure parameters were determined as $D/hc = 0.00598$ cm^{-1} and $E/hc = 0$ cm^{-1} for $\mathbf{3b}^{2+}$, and $D/hc = 0.00437$ cm^{-1} and $E/hc = 0$ cm^{-1} for $\mathbf{4b}^{2+}$. The D/hc value for the *m*-phenylene $\mathbf{3b}^{2+}$

(16) Sun, D.; Rosokha, S. V.; Kochi, J. K. *J. Am. Chem. Soc*. **2004**, *126*, 1388−1401.

(17) (a) Okamoto, T.; Terada, E.; Kozaki, M.; Uchida, M.; Kikukawa, S.; Okada, K. *Org. Lett*. **2003**, *5*, 373−376. (b) Hiraoka, S.; Okamoto, T.; Kozaki, M.; Shiomi, D.; Sato, K.; Takui, T.; Okada, K. *J. Am. Chem. Soc.* **2004**, *126*, 58−59.

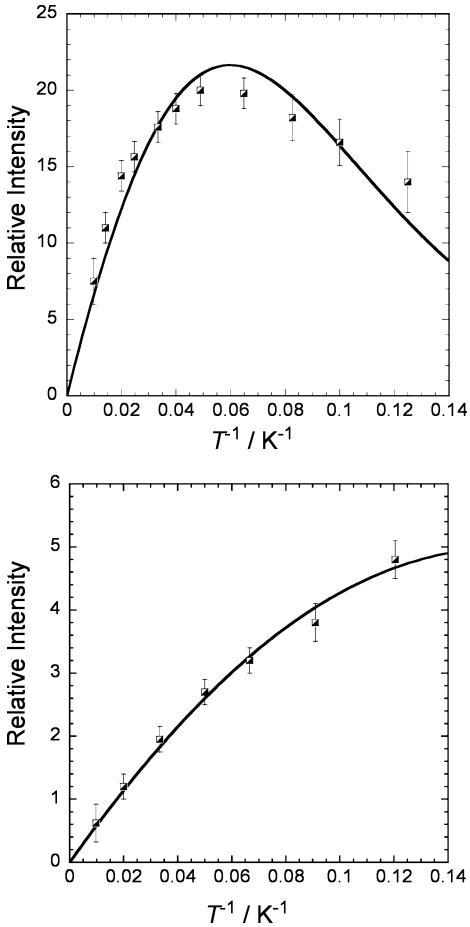

FIGURE 2. Temperature dependence of the EPR signal intensity ($|\Delta m_s| = 2$) for $\mathbf{3b}^{2+}$ (upper) and $\mathbf{4b}^{2+}$ (lower) measured at microwave power = 0.1 mW in a butyronitrile matrix.

is larger than that for the *p*-phenylene $\mathbf{4b}^{2+}$, indicating that the averaged distance between the spin centers is shorter for the *m*-phenylene $\mathbf{3b}^{2+}$ (7.5 Å from the point dipole approximation) than that for the *p*-phenylene $\mathbf{4b}^{2+}$ (8.7 Å). The calculated distance is close to the distance between the two centers of the dihydrophenazine rings (ca 7.5 Å for the *m*-isomer and 8.6 Å for the *p*-isomer). Similar *D*/*hc* values were observed for $\mathbf{3a}^{2+}$ (0.00598 cm^{-1}) and $\mathbf{4a}^{2+}$ (0.00449 cm^{-1}) (Figure S2).

A weak forbidden signal for the $|\Delta m_s| = 2$ transition was observed in lower temperatures for these compounds. Figure 2 shows the temperature dependence of the signal intensity (I) of the $|\Delta m_s| = 2$ transition. The plots (I vs T^{-1}) for the *m*-isomer $\mathbf{3b}^{2+}$ gave a convex curve in the temperature region between 8.0 and 102 K. Simulation with the ST model indicated a singlet ground state with $\Delta E_{ST}/k_B = -27 \pm 1$ K (solid line in Figure 2). A similar value was obtained for $\mathbf{3a}^{2+}$ ($\Delta E_{ST}/k_B = -21 \pm 1$ K, Figure S3). The absolute values of these are somewhat larger than the value ($\Delta E_{ST}/k_B = -14$ K) for the previously reported *m*-phenylenebis(phenothiazine) dication $\mathbf{1}^{2+}$.[8a]

Similar plots for the *p*-isomer $\mathbf{4b}^{2+}$ gave a slightly curved line (Figure 2 (lower)) in the temperature range between 8.3 and 103 K with microwave power = 0.1 mW. To avoid saturation of signal intensity, microwave power dependence (0.01, 0.1, 0.49, 1 mW) of the signal intensity was studied. The signal intensity vs the square root of microwave power gave a straight line (Figure S4, lower). Therefore, the observed curvature for $\mathbf{4b}^{2+}$ is not due to the saturation of the signal but due to the low-spin ground-state nature. The plots were simulated as a singlet ground state with $\Delta E_{ST}/k_B = -9.6 \pm 1.0$ K. Similar plots for the 10,10′-diphenyl derivative $\mathbf{4a}^{2+}$ (Figure S3, lower) also indicate the curvature with $\Delta E_{ST}/k_B = -8.6 \pm 0.3$ K. For these reasons, it can be concluded that the *p*-isomers $\mathbf{4}^{2+}$ have a singlet ground state with $|\Delta E_{ST}/k_B|$ as small as 8−10 K.

It should be noted that the previously reported (*p*-phenylene)bis(phenothiazines) dications $\mathbf{2}^{2+}$ gave a straight line in the temperature range between 6 and 60 K. The plots passed through the origin and no tendency of curvature was observed,[8a] suggesting a triplet ground state or a singlet ground state with $|\Delta E_{ST}/k_B| < \sim 6$ K.

We have also examined the measurement of magnetic susceptibility for the powdered samples of 5,5′-(*m*- and *p*-phenylene)bis[10-(4-butylphenyl)-5,10-dihydrophenazine]s, $\mathbf{3b}^{2+}(SbCl_6^-)_2 \cdot C_6H_6$ and $\mathbf{4b}^{2+}(SbCl_6^-)_2$. Attempts to dilute these dications in PVC films to extract intramolecular magnetic interactions failed to give a homogeneous film because of their poor solubility in organic solvents. The measurement for the powdered samples prevented the precise analysis of the magnetic interactions because of the presence of intermolecular magnetic interactions and of the lack of the crystal structure that is essential for making a theoretical model for analysis. Nevertheless, qualitative features for the magnetic susceptibility study[18] for the powdered samples were consistent with the EPR studies. The description of the study for magnetic susceptibility is provided in Supporting Information.

Computational Analysis 1. Exchange Interaction. The (*m*- and *p*-phenylene)bis(phenothiazine) dications, $\mathbf{1}^{2+}$ and $\mathbf{2}^{2+}$, and the bis(dihydrophenazine) dication analogues, $\mathbf{3}^{2+}$ and $\mathbf{4}^{2+}$, have nearly perpendicular geometries between the plane of the central phenylene ring and the spin sources, judging from the X-ray structure of the related analogues.[17b,19] At perpendicular geometry, the π (spin source)−π (phenylene)−π (spin source) orbital interaction is completely forbidden, whereas the $\pi-\sigma-\pi$ type orbital interaction is permitted. Although such a tightly perpendicular condition is unrealistic, theoretical insight into this extreme case is quite useful to understand the origin of the magnetic interaction of these dications. The orbital and magnetic interactions through the σ-frame of *m*-phenylene has already been demonstrated for (*m*-phenylene)bisnitroxide by Borden and coworkers.[11] However, such an approach for the *p*-phenylene system has not been reported. We consider here the magnetic and orbital interactions at exactly perpendicular geometries (C_{2v} symmetry for *m*-isomers and D_{2h}

(18) The intra- and intermolecular magnetic interactions of these dications $\mathbf{3b}^{2+}$ and $\mathbf{4b}^{2+}$ in the crystalline solid state were examined by the paramagnetic susceptibility χ_p on a SQUID magnetometer between 300 and 1.9 K. The diamagnetic susceptibility χ_d of -772×10^{-6} emu mol^{-1} was subtracted from the observed susceptibility for $\mathbf{3b}^{2+}(SbCl_6^-)_2 \cdot C_6H_6$. The contribution of the $SbCl_6^-$ anion to χ_d was estimated by measuring the susceptibility of tetraethylammonium salt of $SbCl_6^-$. The contribution from the other atoms and groups in $\mathbf{3b}^{2+}(SbCl_6^-)_2 \cdot C_6H_6$ was evaluated using Pascal's constants. The same values of the diamagnetic susceptibility χ_d for the cation and the $SbCl_6^-$ anion were applied to the *p*-isomer, $\mathbf{4b}^{2+}(SbCl_6^-)_2$.

(19) Okamoto, T.; Kuratsu, M.; Kozaki, M.; Hirotsu, K.; Ichimura, A.; Matsushita, T.; Okada, K. *Org. Lett.* **2004**, *6*, 3493−3496.

symmetry for *p*-isomers) of bis(dihydrophenazine) dications **3a**$^{2+}$ and **4a**$^{2+}$ and the bis(phenothiazine) dications **1**$^{2+}$ and **2**$^{2+}$. Bis(methylene) diradicals, **6** and **7**, at the perpendicular geometries were also studied as simple models and for comparison with Borden's calculation results (GVB-ROHF and (8/8)CASSCF) for the *m*-isomer **6**.

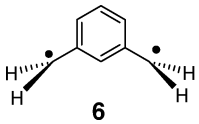

6

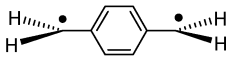

7

The effective exchange integral (J_{ab}) between magnetic sites has been described by the Heisenberg (HB) model on experimental grounds as

$$H(\mathrm{HB}) = -2\sum J_{ab}\mathbf{S_a}\cdot\mathbf{S_b} \tag{1}$$

where $\mathbf{S_a}$ and $\mathbf{S_b}$ are spins at sites **a** and **b**, respectively. The recent development of computational techniques involving the calculation of open-shelled species has enabled estimation of the J_{ab} values for various systems.[17b,20−26] In particular, UHF methods have been found to be effective for large molecular systems. When one applies UHF methods to diradical systems, the default initial guess for singlet states often fails to give a correct answer. The magnetic orbitals (α and β) of a singlet state are typically expressed as a linear combination (in-phase or out-of-phase with keeping the symmetry) of the localized orbitals at radical sites. However, for certain diradical systems, particularly those with weak overlap between two localized orbitals, their magnetic orbitals (α and β) are well approximated such that the α spin occupies mainly one of the radical sites and the β-spin occupies mainly the other site. Such a state has unsymmetrical spin and spatial symmetry even if the diradical has a symmetrical geometry. Such a broken-symmetry (BS) state frequently gives lower energy than the state with symmetry-adopted magnetic orbitals, simply because the electronic repulsion of the former system would be minimized as a result of the different region of space between α and β spins. According to Davidson, the energy and geometry thus obtained are precise enough and comparable to CASSCF calculation in some simple molecules.[26] The UHF state calculated using the SCF procedure exhibits spin-contamination contributed from higher spin states. Therefore, establishing a suitable spin-projection procedure is also essential. There are currently three formulizations that can be used to estimate J_{ab} values:[20−23]

$$J_{ab}^{(1)} = \frac{^{LS}E - {}^{HS}E}{S_{max}^2} \tag{2}$$

$$J_{ab}^{(2)} = \frac{^{LS}E - {}^{HS}E}{S_{max}(S_{max}+1)} \tag{3}$$

$$J_{ab}^{(3)} = \frac{^{LS}E - {}^{HS}E}{\langle {}^{HS}S^2\rangle - \langle {}^{LS}S^2\rangle} \tag{4}$$

where ^{LS}E, ^{HS}E, and S_{max} are, respectively, the total energies of the low-spin and high-spin states, and the maximum spin number of the system. The $J_{ab}^{(1)}$ value is applicable to systems with a small overlap between magnetic orbitals.[21] The $J_{ab}^{(2)}$ value is suitable for systems with a relatively large overlap.[20,22] The $J_{ab}^{(3)}$ value varies between the $J_{ab}^{(1)}$ and $J_{ab}^{(2)}$ values depending on the overlap.[20,23]

C_{2v} symmetry was adopted for the *m*-isomers during the geometrical optimization (UB3LYP/6-31G(d)), whereas D_{2h} symmetry was adopted for the *p*-isomers for both the triplet and the BS-singlet states. Under this restriction, pyramidalization at the spin center is allowed but the π-orbital of the spin center can only interact with the σ-orbitals of the central ring. The optimized geometries were nearly identical between the triplet state and the BS-singlet state for **1**$^{2+}$, **3a**$^{2+}$, **6**, and **7** and were exactly identical for **2**$^{2+}$ and **4a**$^{2+}$ (Table S1).

Table 1 shows the calculated total energy (UB3LYP/6-31G(d)) of the lowest singlet and triplet states and the exchange interactions for **1**$^{2+}$, **2**$^{2+}$, **3a**$^{2+}$, **4a**$^{2+}$, **6**, and **7**. The $J^{(2)}$ value of the model compound **6** is close to the reported values, GVB-ROHF ($J/k_B = -65$ K) and (8/8)-CASSCF ($J/k_B = -45$ K) for **6**,[11] indicating the validity of the present approach. All of the *m*-isomers have a singlet ground state. The calculated *J* values can be compared to the experimentally determined ΔE_{ST} values with the relation of $\Delta E_{ST} = 2J$, showing good agreement in their orders between the theoretical and experimental values for the *m*-isomers.

The *p*-phenylene dications **2**$^{2+}$ and **4a**$^{2+}$ also have singlet ground states and the absolute values of *J* are considerably smaller than the experimental values. The *p*-phenylenebismethylene **7** has a singlet ground state; the $|J|$ of **7** is larger than those of **2**$^{2+}$ and **4a**$^{2+}$ and smaller than that of **6**.

The calculated *J* values do not relate to the spin density at benzylic position nor the energy difference between the two magnetic orbitals in the BS-singlet state, $\Delta E_{SMO} = |\mathrm{HOMO}(\alpha) - \mathrm{HOMO}-1(\beta)|$, although there is a precedent that the square of spin density correlates to *J* values in a series of substituted *m*-phenylene diradicals.[24c] Importantly, however, the energy difference between the two magnetic orbitals in the triplet state, $\Delta E_{TMO} = |\mathrm{HOMO}(\alpha) - (\mathrm{HOMO}-1)(\alpha)|$ well correlates to the calculated exchange interactions (Table 2 and Figure 3). Per computational interpretation, the qualitative

(20) Ginsberg, A. P. *J. Am. Chem. Soc*. **1980**, *102*, 111−117.
(21) (a) Noodleman, *J. Chem. Phys*. **1981**, *74*, 5737−5743. (b) Noodleman, L.; Davidson, E. R. *Chem. Phys*. **1986**, *109*, 131−143. (c) Bencini, A.; Totti, F.; Daul, C. A.; Doclo, K.; Fantucci, P.; Barone, V. *Inorg. Chem.* **1997**, *36*, 5022−5030. (d) Eklund, J. C.; Bond, A. M.; Colton, R.; Humphrey, D. G.; Mahon, P. J.; Walter, J. W. *Inorg. Chem*. **1999**, *38*, 2005−2011.
(22) Ruiz, E.; Cano, J.; Alvarez, S.; Alemany, P. *J. Comput. Chem*. **1999**, 1391−1400.
(23) (a) Yamaguchi, K.; Fukui, H.; Fueno, T. *Chem. Lett*. **1986**, 625−628. (b) Yamaguchi, K.; Jensen, F.; Dorigo, A.; Houk, K. N. *Chem. Phys. Lett*. **1988**, 149, 537−542. (c) Yamaguchi, K.; Yamaguchi, K. *Int. J. Quantum Chem*. **2002**, *90*, 370−385. (d) Okada, K.; Nagao, O.; Mori, H.; Kozaki, M.; Shiomi, D.; Sato, K.; Takui, T.; Kitagawa, Y.; Yamaguchi, K. *Inorg. Chem.* **2003**, *42*, 3221−3228.
(24) (a) Lahti, P. M.; Ichimura, A. S.; Sanborn, J. A. *J. Phys. Chem. A* **2001**, *105*, 251−260. (b) Zhang, G. B.; Li, S. H.; Jiang, Y. S. *J. Phys. Chem. A* **2003**, *107*, 5573−5582. (c) Zhang, G.; Li, S.; Jiang, Y. *Tetrahedron* **2003**, *59*, 3499−3504. (d) Constantinides, C. P.; Koutentis, P. A.; Schatz, J. *J. Am. Chem. Soc*. **2004**, *126*, 16232−16241.
(25) Gräfenstein, J.: Kraka, E.; Filatov, M.; Cremer, D. *Int. J. Mol. Sci*. **2002**, *3*, 360−394.
(26) Davidson, E. R. *Int. J. Quantum Chem*. **1998**, *69*, 241−245.

TABLE 1. Calculated Total Energies and Effective Exchange Integrals for 1^{2+}, 2^{2+}, $3a^{2+}$, $4a^{2+}$, 6, and 7

compd	BS-singlet state energy/hartree	BS-singlet state $\langle S^2\rangle$	triplet state energy/hartree	triplet state $\langle S^2\rangle$	ground state	Jk_B^{-1}/K $J^{(1)}/k_B$	$J^{(2)}/k_B$	$J^{(3)}/k_B$	$\Delta E_{ST}k_B^{-1}$, $2Jk_B^{-1}$/K (experimental value)
1^{2+}	−2060.58260279	1.0105	−2060.58255600	2.0132	BS-singlet	−14.8	−7.4	−14.7	−14[a]
2^{2+}	−2060.58565647	1.0130	−2060.58565368	2.0132	BS-singlet	−0.88	−0.44	−0.88	> −6[a]
$3a^{2+}$	−1837.07394913	1.0126	−1837.07391262	2.0146	BS-singlet	−11.5	−5.8	−11.5	−27 to −21
$4a^{2+}$	−1837.07698935	1.0144	−1837.07698694	2.0146	BS-singlet	−0.76	−0.38	−0.76	−10 to −8
6	−309.536938545	1.0012	−309.536588055	2.0079	BS-singlet	−110.7	−55.3	−109.9	[b]
7	−309.536976973	1.0052	−309.536778357	2.0075	BS-singlet	−62.7	−31.4	−62.6	[b]

[a] Refrence 7a. [b] Unknown.

TABLE 2. Orbital Energies at HOMO and HOMO-1 in the BS-Singlet and Triplet States for 1^{2+}, 2^{2+}, $3a^{2+}$, $4a^{2+}$, 6, and 7

compd	BS-singlet state/hartree HOMO (α)	HOMO (β)	ΔE_{SMO}	spin density at benzylic position	triplet state/hartree HOMO (α)	HOMO-1 (α)	ΔE_{TMO}	$\Delta E_{TMO}k_B^{-1}$/K
1^{2+}	−0.41294	−0.41294	0.00000	+0.246674	−0.41186	−0.41404	0.00218	688
2^{2+}	−0.40926	−0.40926	0.00000	+0.245612	−0.40899	−0.40953	0.00054	171
$3a^{2+}$	−0.37821	−0.37821	0.00000	+0.231390	−0.37717	−0.37928	0.00211	666
$4a^{2+}$	−0.37494	−0.37494	0.00000	+0.230977	−0.37467	−0.37522	0.00055	174
6	−0.21588	−0.21558	0.00000	+1.129724	−0.21023	−0.22188	0.01165	3679
7	−0.21593	−0.21593	0.00000	+1.127627	−0.21272	−0.21918	0.00646	2037

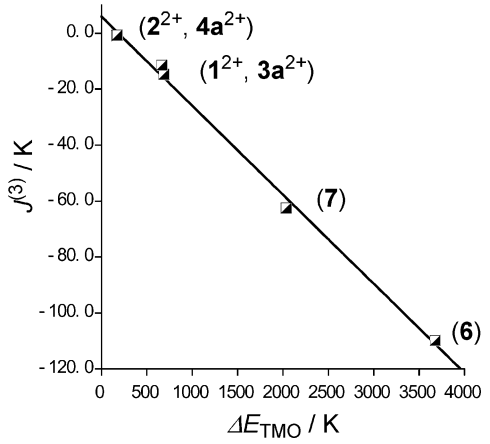

FIGURE 3. Plots of $J^{(3)}$ values to the MO energy difference in the triplet states, $\Delta E_{TMO} = |(HOMO(\alpha) - (HOMO-1)(\alpha))|$, for 1^{2+}, 2^{2+}, $3a^{2+}$, $4a^{2+}$, 6, and 7.

relationship between J and orbital splitting between magnetic orbitals is well-known.[11] Importantly, however, the $J^{(3)}$ values for both *m*- and *p*-isomers can be approximated as a single straight line expressed by eq 5 with a good correlation factor ($R = 0.998$):

$$J^{(3)} = A - B\cdot\Delta E_{TMO} \quad (5)$$

where $A/k_B = 6.0 \pm 1.7$ K and $B = 0.032 \pm 0.001$. The single straight line suggests that the topological difference is minimized at the perpendicular geometry. Although J values are dependent on the estimation methods ($J^{(1)}$, $J^{(2)}$, and $J^{(3)}$) and also on the theoretical methodologies,[11] the difference is likely to be systematic. The good correlation obtained by the identical method suggests the generality of this relationship at the perpendicular geometry. The positive A value corresponds to the ferromagnetic interaction expected for the complete degenerate magnetic orbitals systems. B is a scaling factor. This correlation between the J values and ΔE_{TMO} values allows interpretation of the exchange interaction in terms of molecular orbital interaction in the triplet states. We discuss the exchange interaction for these compounds in the sense of molecular orbital interaction.

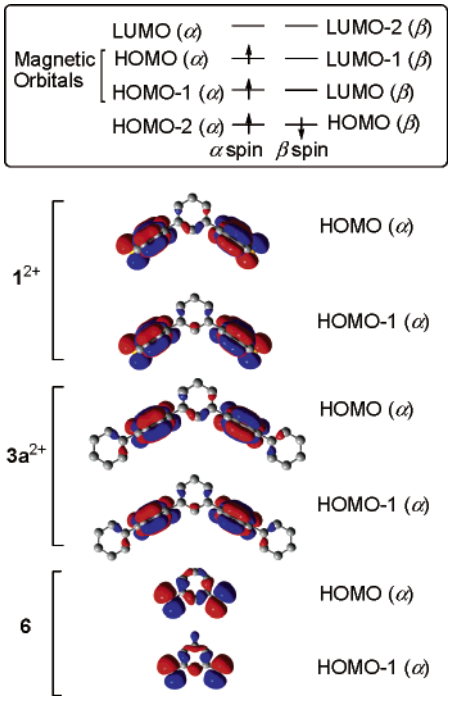

FIGURE 4. Schematic energy diagram (UHF presentation) and MO shape of the triplet states for 1^{2+}, $3a^{2+}$, and 6.

Computational Analysis 2. Exchange Interaction through MO interaction. The shapes of magnetic orbitals, HOMO(α) and (HOMO − 1)(α), in the triplet state for the *m*-isomers are shown in Figure 4. The mixing of the σ-orbital of the *m*-phenylene moiety is clearly seen. Schematic diagrams of the orbital interaction for the *m*-isomers are shown in Figure 5. Both symmetric and antisymmetric orbitals (π_S and π_A, Figure 5) are destabilized by the mixing of σ-orbitals (σ_{S1} and σ_{A1}) of the central ring. Because of the suitable orientation of the 2*p* atomic orbital at the C2 in the *m*-phenylene, the mixing coefficient a of the antisymmetric σ-orbital (σ_{A1}) is larger than that (a') of the symmetric σ-orbital

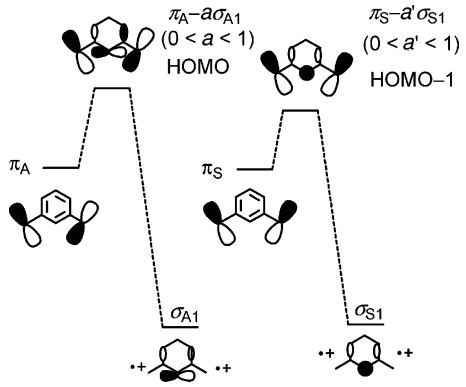

FIGURE 5. MO-interaction diagram for *m*-phenylene dications.

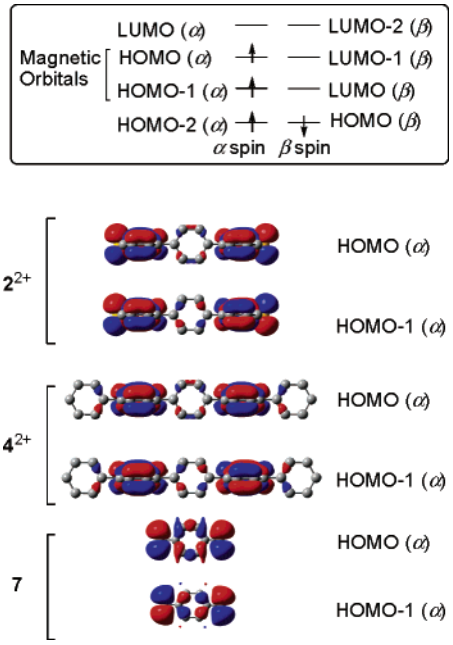

FIGURE 6. Energy diagram (UHF presentation) and MO shape of the triplet states for $\mathbf{2}^{2+}$, $\mathbf{4a}^{2+}$, and **7**.

(σ_{S1}), thus leading to the antisymmetric $\pi_A - a\sigma_{A1}$ ($0 < a' < a < 1$) as a higher orbital, HOMO (α). This orbital splitting favors a singlet ground state. This situation is quite similar to that observed in Borden's study for (*m*-phenylene)bisnitroxides.[11] The *m*-phenylene diradical **6** has larger mixing coefficients of the σ-orbitals, which expand the orbital splitting (ΔE_{TMO}), resulting in a large $|J|$.

The smaller ΔE_{TMO} values for the *p*-isomers mainly reflect the longer five σ-bonds between the two spin sources. The shape of magnetic orbitals in the triplet state for the *p*-isomers is shown in Figure 6, and their orbital interaction diagram is given in Figure 7. It is interesting to note that there is a large difference in the symmetry nature of HOMO between the *p*- and *m*-isomers, i.e., symmetric HOMO for the *p*-isomers and antisymmetric HOMO for the *m*-isomers. As shown in the case of the *m*-isomers, both symmetric and antisymmetric orbitals (π_S and π_A) are destabilized by the mixing of σ-orbitals (σ_{S1}, σ_{S2}, and σ_{A1}) of the central ring. In the *p*-isomers, the symmetric orbital ($\pi_S - a\sigma_{S1}$, $0 < a < 1$) selectively receives further destabilization from the

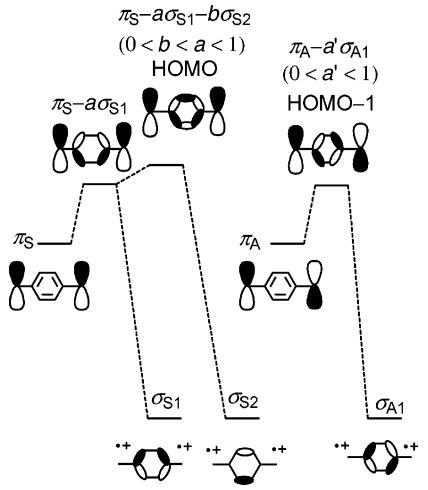

FIGURE 7. MO-interaction diagram for *p*-phenylene dications.

central C_2-C_3 bond (σ_{S2}) of the *p*-phenylene moiety. However, such participation of the C_2-C_3 bond (σ_{S2}-orbital) is absent in the antisymmetric orbital ($\pi_A - a'\sigma_{A1}$, $0 < a' < 1$). Thus, the symmetrical orbital ($\pi_S - a\sigma_{S1} + b\sigma_{S2}$, $0 < b < a < 1$) is pushed up as a HOMO (α). The contribution of the remote C_2-C_3 bond should be small since the coefficient *b* is a mixing coefficient of the small $a\sigma_{S1}$-orbital and appears as a small lobe in the HOMO (α) (Figure 6), resulting in a small energy gap between HOMO(α) and (HOMO − 1) (α).

Generally speaking, the energy gap between two magnetic orbitals favors singlet states. However, the nondisjoint nature of these magnetic orbitals causes an extra electronic repulsion in the singlet state: the BS-approach estimates the most stable singlet energy by minimizing such electronic repulsion. Such electronic repulsion is absent in the triplet state because of the inherent triplet nature. For this reason, when the energy gap between the magnetic orbitals is small, the disadvantage in energy of the triplet state due to the orbital energy gap (ΔE_{TMO}) may be compensated by the electronic repulsion in the singlet state, giving the triplet and singlet states in a nearly degenerate level ($\Delta E_{ST}/k_B = 2J/k_B$ = ca. −2 K for $\mathbf{2}^{2+}$ and $\mathbf{4}^{2+}$). When the orbital splitting becomes larger as in the case of **7**, the electronic repulsion in the singlet state cannot compensate the instability of the triplet state, giving the larger negative ΔE_{ST}.

The observed ΔE_{ST} values for the *m*-dications, $\mathbf{1}^{2+}$ and $\mathbf{3}^{2+}$, are in good agreement with the calculated $2J$ values in their orders, whereas those for the *p*-dications, $\mathbf{2}^{2+}$ and $\mathbf{4}^{2+}$, are considerably larger than the theoretical values. This may be due to the strongly antiferromagnetic nature of the *p*-isomers at nonperpendicular geometries and the small deviation of the torsion angle from the hypothetical perpendicular geometry may rationalize the experiments. Despite the considerably rough treatment with the perpendicular geometry for these dications, the present calculation well explains why the *p*-dications have smaller negative ΔE_{ST} values than the *m*-dications.

Experimental Section

In Situ Preparation of 5-Phenyl-5,10-dihydrophenazine (5a). Into a Schlenk tube containing a phenazine (1.44 g (8.00 mmol)) solution in 8 mL of *o*-xylene was added dropwise

a cyclohexanes−ether mixed solution of phenyllithium (1.06 M, 11 mL) at room temperature under nitrogen. The color of the solution turned dark brown during the addition. The reaction mixture was stirred for 3.5 h and quenched by addition of deaerated distilled water (ca. 20 mL) at 0 °C. The organic layer was transferred via a syringe into another Schenk tube containing dry sodium sulfate (ca. 4 g) under nitrogen. This solution containing **5a** (>70%) can be stored in a refrigerator for a long time.

Preparation of 5,5′-(*m*-Phenylene)bis(10-phenyl-5,10-dihydrophenazine) (3a). A 6.3 mL (ca. 2.5 mmol) solution of thus prepared 5-phenyl-5,10-dihydrophenazine was taken in a 10 mL two-necked flask containing 349 mg (1.06 mmol) of *m*-diiodobenzene, sodium *tert*-butoxide 306 mg (3.18 mmol), 4.7 mg (0.021 mmol) of palladium acetate, and a 0.1 mL (0.017 mmol) of solution of tri-*tert*-butylphosphin in *o*-xylene (0.17 M) under a nitrogen atmosphere. The mixture was heated at 120 °C for 1 h. After cooling to room temperature, the mixture was filtered. The solid part was washed with ca. 10 mL of hot toluene and the filtrate was combined. After evaporation of the solvent, the residue was subjected to aluminum chromatography (hexane−toluene = 3:1), giving the desired **3a** (388 mg, 0.657 mmol, 62% based on *m*-diiodobenzene) as a pale yellow solid: pale yellow powder (recrystallized from tetrahydrofuran−methanol), mp 263 °C; ^{1}H NMR (400 MHz, C_5D_5N) δ 7.90 (t, 1H, J = 8.0 Hz), 7.67−7.60 (m, 4H), 7.60−7.53 (partially overlapped with the solvent signals (m), 2H), 7.51−7.44 (m, 7H), 6.48−6.38 (m, 8H), 5.99 (dd, 4H, J = 7.6, 1.7 Hz), 5.86 (dd, 4H, J = 7.6, 1.7 Hz); IR (KBr, cm^{-1}) 3051, 2968, 2851, 1585, 1485,1346, 1285, 1267, 1061, 733, 698; HRMS (FAB$^+$) calcd for $C_{42}H_{30}N_4$ (M^+) 590.2470, found 590.2473.

Preparation of 5,5′-(*m*-Phenylene)bis(10-phenyl-5,10-dihydrophenazine) Bis(radical cation) (3a^{2+}). The following procedures were achieved in a glovebox. The neutral compound **3a** (10 mg, 0.017 mmol) was dissolved in dry acetonitrile (25 mL). To this solution was slowly added an acetonitrile solution (5 mL) of tris(*p*-bromophenylaminium hexachloroantimonate (42.0 mg, 0.034 mmol). The yellow color solution of **3a** turned green. The acetonitrile solution was concentrated to a minimum amount to dissolve the green solid. Addition of an excess of dry ether into the acetonitrile solution gave **3a**$^{2+}$ as green precipitates (16 mg, 76%): mp 176 °C; IR (KBr, cm^{-1}) 3072, 1589, 1549, 1464, 1344, 1283, 756, 694, 610; HRMS (FAB$^+$) calcd for $C_{42}H_{30}N_4$ (M^+) 590.2471, found 590.2468, HRMS (FAB$^-$) calcd for $SbCl_6^-$ 330.7169, found 330.7173. Anal. Calcd for $C_{42}H_{30}Cl_{12}N_4Sb_2$: C 40.05, H 2.40, N 4.45. Found: C 39.85, H 2.54, N 4.38.

Preparation of 5,5′-(*p*-Phenylene)bis(10-phenyl-5,10-dihydrophenazine) (4a). This compound was prepared according to a similar procedure as for the synthesis of **3a** using *p*-diiodobenzene instead of *m*-diiodobenzene (41% yield): a pale yellow powder (recrystallized from toluene); mp >300 °C; ^{1}H NMR (400 MHz, C_5D_5N) δ 7.72 (s, 4H, J = 8.0 Hz), 7.65−7.60 (m, 4H), 7.51−7.40 (m, 6H), 6.45−6.41 (m, 8H), 6.08−6.04 (m, 4H), 5.88−5.84 (m, 4H); IR (KBr, cm^{-1}) 3063, 3032, 1591, 1477, 1346, 1337, 1283, 1265, 727, 698; HRMS (FAB$^+$) calcd for $C_{42}H_{30}N_4$ (M^+) 590.2470, found 590.2476.

Preparation of 5,5′-(*p*-Phenylene)bis(10-phenyl-5,10-dihydrophenazine) Bis(radical cation) (4a^{2+}). The following procedures were achieved in a glovebox. The neutral compound **4a** (10 mg, 0.017 mmol) was dissolved in dry THF (50 mL). To this solution was slowly added an acetonitrile solution (5 mL) of tris(*p*-bromophenylaminium hexachloroantimonate (42 mg, 0.034 mmol). The yellow color solution of **4a** turned green. The acetonitrile solution was concentrated to a minimum amount to dissolve the green solid. Addition of an excess of dry ether into the acetonitrile solution gave **4a**$^{2+}$ as green precipitates (14 mg, 66%): mp 255 °C; IR (KBr, cm^{-1}) 3057, 2972, 2947, 1553, 1464, 1344, 1283, 752, 704, 692, 611; HRMS (FAB$^+$) calcd for $C_{42}H_{30}N_4$ (M^+) 590.2471, found 590.2468; HRMS (FAB$^-$) calcd for $SbCl_6^-$ 330.7169, found 330.7173. Anal. Calcd for $C_{42}H_{30}Cl_{12}N_4Sb_2$: C 40.05, H 2.40, N 4.45. Found: C 39.94, H 2.50, N 4.41.

In Situ Preparation of 5-(4-*n*-Butylphenyl)-5,10-dihydrophenazine (5b). In a Schlenk tube was charged a 2.94 g (16.3 mmol) of phenazine and 15 mL of toluene. To this solution was added dropwise an 8.1 mL solution of 4-*n*-butylphenyllithium (0. 85 M), prepared from 1-bromo-4-*n*-butylbenzene and lithium metal. The resulting dark-brown mixture was stirred for 3.5 h and quenched by addition of deaerated distilled water (ca. 20 mL) at 0 °C. The organic layer were transferred via a syringe into another Schenk tube containing dry sodium sulfate (ca 4 g) under nitrogen. This solution **5b** (>70%) can be stored in a refrigerator for a long time.

Preparation of 5,5′-(*m*-Phenylene)bis[10-(4-*n*-butylphenyl)-5,10-dihydrophenazine] (3b). This compound was prepared according to a similar procedure as for the synthesis of **3a** using 5-(4-*n*-butylphenyl)-5,10-dihydrophenazine instead of 5-phenyl-5,10-dihydrophenazine (69% yield): pale yellow powder (recrystallized from benzene−methanol); mp 179 °C; ^{1}H NMR (400 MHz, C_5D_5N) δ 7.91 (t, 1H, J = 8.0 Hz), 7.59−7.56 (overlapped with the solvent peak, 2H), 7.50 (s, 1H), 7.49−7.39 (AA′BB′, 8H), 6.48−6.38 (m, 8H), 6.01 (dd, 4H, J = 7.3, 2.0 Hz), 5.93 (dd, 4H, J = 7.3, 2.0 Hz), 2.66 (t, 4H, J = 7.8 Hz), 1.65−1.55 (m, 4H), 1.37−1.27 (m, 4H), 0.89 (t, 6H, J = 7.3 Hz); IR (KBr, cm^{-1}) 3053, 3026, 2954, 2928, 2858, 1585, 1485, 1346, 1285, 1267, 729; HRMS (FAB$^+$) calcd for $C_{50}H_{46}N_4$ (M^+) 702.3722, found 702.3752.

Preparation of 5,5′-(*m*-Phenylene)bis[10-(4-*n*-butylphenyl)-5,10-dihydrophenazine] Bis(radical cation) (3b^{2+}). The following procedures were achieved in a glovebox. The neutral compound **3b** (50 mg, 0.071 mmol) was dissolved in dry acetonitrile (2 mL). To this solution was slowly added an acetonitrile solution (10 mL) of tris(*p*-bromophenyl)aminium hexachloroantimonate (115 mg, 0.141 mmol). The yellow color solution of **3b** turned green. The acetonitrile solution was concentrated to a minimum amount to dissolve the green solid. Addition of an excess of dry ether into the acetonitrile solution gave **3b**$^{2+}$ as green precipitates (75 mg, 73%), which can be recrystallized from acetonitrile−benzene: mp 161 °C; IR (KBr, cm^{-1}) 3060, 2960, 2928, 2858, 1589, 1549, 1466, 1342, 1282, 1189, 1160, 752, 677, 606; MS (FAB$^+$) calcd for $C_{50}H_{46}N_4$ (M^+) 702, found 702; MS (FAB$^-$) calcd for $SbCl_6^-$ 331, found 331. Anal. Calcd for $C_{50}H_{46}Cl_{12}N_4Sb_2{\cdot}C_6H_6$: C 46.39, H 3.61, N 3.86. Found: C 46.09, H 3.49, N 3.87.

Preparation of 5,5′-(*p*-Phenylene)bis[10-(4-*n*-butylphenyl)-5,10-dihydrophenazine] (4b). This compound was prepared according to a similar procedure as for the synthesis of **3a** using 5-(4-*n*-butylphenyl)-5,10-dihydrophenazine and *p*-diiodobenzene instead of 5-phenyl-5,10-dihydrophenazine and *m*-diiodobenzene, respectively (68% yield): pale yellow powder (recrystallized from toluene); mp >300 °C; ^{1}H NMR (400 MHz, C_5D_5N) δ 7.74 (s, 4H), 7.50−7.34 (AA′BB′, 8H), 6.52−6.37 (m, 8H), 6.11−6.03 (m, 4H), 5.97−5.90 (m, 4H), 2.66 (t, 4H, J = 7.8 Hz), 1.65−1.55 (m, 4H), 1.37−1.27 (m, 4H), 0.89 (t-like, 6H, J = ca. 7 Hz); IR (KBr, cm^{-1}) 3063, 3030, 2956, 2930, 2856, 1601, 1483, 1348, 1286, 1267, 731; HRMS (FAB$^+$) calcd for $C_{50}H_{46}N_4$ (M^+) 702.3722, found 702.3745.

Preparation of 5,5′-(*p*-Phenylene)bis[10-(4-*n*-butylphenyl)-5,10-dihydrophenazine] Bis(radical cation) (4b^{2+}). The following procedures were achieved in a glovebox. The neutral compound **4b** (50 mg, 0.071 mmol) was dissolved in dry THF (110 mL). To this solution was slowly added an acetonitrile solution (15 mL) of tris(*p*-bromophenyl)aminium hexachloroantimonate (118 mg, 0.145 mmol). The yellow color solution of **4b** turned green. The acetonitrile solution was concentrated to a minimum amount to dissolve the green solid. Addition of an excess of dry ether into the acetonitrile solution gave **4b**$^{2+}$ as green precipitates (70 mg, 72%), which can be recrystallized from acetonitrile−benzene: mp 226 °C; IR (KBr, cm^{-1}) 3059, 2955, 2930, 2856, 1607, 1555, 1506, 1466, 1348, 1283, 1186, 1161, 745, 613; MS (FAB$^+$) calcd for $C_{50}H_{46}N_4$ (M^+)

702, found 702; MS (FAB$^-$) calcd for $SbCl_6^-$ 331, found 331. Anal. Calcd for $C_{50}H_{46}N_4Sb_2Cl_{12}$: C 43.77, H 3.38, N 4.08. Found: C 43.50, H 3.28, N 3.89.

Calculation Method. The Gaussian 03 program package was used in this study. The criterion for the SCF convergence was 10^{-9}. For the calculation of the low-spin BS singlet states, a trial wave function for the SCF procedure was generated by the HOMO−LUMO mixing using the keyword "mix".

Acknowledgment. We thank the Ministry of Education, Culture, Sports, Science and Technology, Japan, for a Grant-in-Aid for Scientific Research (nos. 17350072, 17350073). One of the authors (D.S.) acknowledges financial support from PRESTO of Japan Science and Technology Agency (JST).

Supporting Information Available: Cyclic voltammogram charts for **3a**,**b** and **4a**,**b** (Figure S1), EPR spectra for $\mathbf{3a}^{2+}$ and $\mathbf{4a}^{2+}$ and the simulation spectra (Figure S2), Curie plots of the EPR signal intensity ($|\Delta m_s| = 2$) for $\mathbf{3a}^{2+}$ and $\mathbf{4a}^{2+}$ (Figure S3), microwave power dependence of EPR signal intensity (Figure S4), the study of the magnetic susceptibility for $\mathbf{3b}^{2+}$ and $\mathbf{4b}^{2+}$ (Figure S5 and Figure S6), the MOs in BS-singlet states for the *m*-isomers, $\mathbf{1}^{2+}$, $\mathbf{3a}^{2+}$, and **6** (Figure S7) and for the *p*-isomers, $\mathbf{2}^{2+}$, $\mathbf{4a}^{2+}$, and **7** (Figure S8), and the Cartesian coordinates of the optimized geometries in the triplet and BS-singlet states for $\mathbf{1}^{2+}$, $\mathbf{2}^{2+}$, $\mathbf{3a}^{2+}$, $\mathbf{4a}^{2+}$, **6**, and **7** (Table S1). This material is available free of charge via the Internet at http://pubs.acs.org.

JO051791W